Transverse collective motion in intermediate-energy heavy-ion collisions

C. A. Ogilvie, D. A. Cebra, J. Clayton, P. Danielewicz,* S. Howden, J. Karn,
A. Nadasen,† A. Vander Molen, G. D. Westfall, W. K. Wilson, and J. S. Winfield
National Superconducting Cyclotron Laboratory and Department of Physics and Astronomy, Michigan State University, East Lansing, Michigan 48824

(Received 28 June 1989; revised manuscript received 28 August 1989)

Light charged fragments from the reactions $^{40}Ar+^{51}V$ at 35 MeV/nucleon and $^{12}C+^{12}C$ at 50 MeV/nucleon have been measured with a 4π array. Transverse collective motion is observed for all fragment types and increases in strength for the heavier fragments. The transverse momentum is qualitatively similar for the different impact parameters selected by the midrapidity charge. The global transverse momentum analysis includes corrections for correlations due to momentum conservation. The results are compared to those at higher energies to investigate whether the same or a new reaction phenomenon produces the collective motion. We outline some implications for the extraction of thermodynamic information from the kinetic energy of emitted fragments.

I. INTRODUCTION

Nuclear matter well away from its ground state can be formed during the collision of two nuclei at intermediate bombarding energies. Many studies[1] have attempted to characterize the properties of this matter; whether it has reached local or global equilibrium, and if so, whether the system is describable by its thermodynamic variables, i.e., can we assign a temperature and entropy to the nuclear matter that participates in the collision?

Before reaching a firm understanding of the properties of nuclear matter, we need to know how the collision produces the hot matter, and in particular whether the collision dynamics produces any collective motion within the reacting system. The presence of collective motion can distort the experimental quantities (e.g., energy spectra) that are traditionally used to examine the thermodynamic properties of the excited nuclear system. For example, noncentral collisions may produce rotating hot nuclear matter. There may also exist a directed collective velocity within the reaction plane. In order to extract the properties of the hot colliding matter, one must either understand the effects of the collective motion, or study classes of reactions where the collective motion is small.

A method to study directed collective motion in the reaction plane is the global transverse momentum analysis developed by Danielewicz and Odyniec.[2] Directed collective motion is where the transverse momentum is of opposite direction for fragments emitted in the forward and backward hemispheres of the center-of-mass frame. In this technique, the transverse momentum of each fragment is projected onto an estimated reaction plane for the event. To remove isotropic motion, one calculates the average transverse momentum over many events; this reveals the presence of any directed collective velocity.

The study of collective motion in these collisions should also provide key information on dynamical questions, such as the interplay between the mean-field and nucleon-nucleon collisions at beam energies between 20 and 100 MeV/nucleon. Several years ago, Molitoris *et al.*[3] predicted that at low bombarding energies the directed transverse momentum would correspond to negative angle scattering caused by mean-field effects. This is in contrast to the behavior at higher beam energies ($E > 200$ MeV/nucleon), where the collective motion is understood to correspond to positive angle scattering due to hydrodynamic side-splash effects. Unfortunately, the global transverse momentum analysis cannot determine the overall sign of the directed momentum. However, by examining the results from different beam energies we may be able to infer from the evolution of the magnitude of the data some evidence for a change of the reaction mechanism.

II. EXPERIMENT DETAILS

We have measured light charged fragements from the $^{40}Ar+^{51}V$ reaction at 35 MeV/nucleon, and the $^{12}C+^{12}C$ reaction at 50 MeV/nucleon, with phase I of the MSU 4π array.[4] The beams were provided by the K500 cyclotron of the National Superconducting Cyclotron Laboratory (NSCL). In the phase I configuration of the MSU 4π array there are 45 phoswich detectors in a forward array between $\theta=7°$ and $\theta=20°$, and 170 phoswich detectors in the main detector (the ball) between $\theta=20°$ and $\theta=160°$. The solid angle coverage of the device is 85% of 4π. The gains of the forward array and ball detectors were set to measure fragments with $Z \leq 8$ and $Z \leq 4$, respectively, with isotopic resolution for $Z=1$ particles. The dynamic range for elemental identification is between 15 and 150 MeV/nucleon for the forward array, and 20 to 200 MeV/nucleon for the main detector. The ranges for isotopic identification were 15–75 and 20–100 MeV/nucleon, respectively. Charged nuclei with $Z > 1$ were assigned $A=2Z$. Fragments that stop in the ΔE part of each detector cannot be firmly identified. However, from the ΔE signal we know the minimum charge of the fragment. This charge and an approximate energy

 ©1989 The American Physical Society

were assigned to the fragment. Such particles were used to determine the impact parameter but were not used in the analysis of transverse momentum.

The data presented in this paper have been separated on an event-by-event basis into three impact-parameter groups; central, midcentral, and midperipheral collisions. We have used the midrapidity charge (Z_{mr}) as an impact filter,[5] where Z_{mr} is the sum of the charges of those fragments that fall within the rapidity window

$$0.75y_{targ} < y < 0.75y_{proj} \quad (1)$$

and y is the fragment's rapidity in the center-of-mass frame of the nuclei. The midrapidity-charge gates that we have used, along with the estimated[5] median impact parameter to which each gate corresponds, are listed in Table I. In Sec. III we show that a further cut on the data improves the determination of the reaction plane. The cut corresponds to selection of only those events with at least three fragments above the low-energy thresholds of the device, one of which must be in the backward center-of-mass hemisphere. Different on-line multiplicity triggers are combined in order to lower the statistical errors for the more central events.

III. ANALYSIS

Application of the transverse momentum analysis presumes that the dominant correlation between the fragment's transverse momenta is caused by collective motion within the reaction plane. Under these circumstances, the average correlation of momenta between any two fragments in the event can be written[6]

$$\langle \mathbf{p}^{\perp}(y_1)/A_1 \cdot \mathbf{p}^{\perp}(y_2)/A_2 \rangle = \langle p^x(y_1)/A_1 \rangle \langle p^x(y_2)/A_2 \rangle , \quad (2)$$

where $\mathbf{p}^{\perp}(y)/A$ is the fragment's transverse momentum per nucleon, $\langle p^x(y)/A \rangle$ is the average transverse momentum per nucleon within the reaction plane, and y is the fragment's rapidity. For nuclear reactions between lighter systems ($A \leq 40$), the collective motion may not be dominant and the correlation [Eq. (2)] may be distorted by the restraint of momentum conservation. Danielewicz *et al.*[6] have shown that momentum conservation modifies Eq. (2) to yield

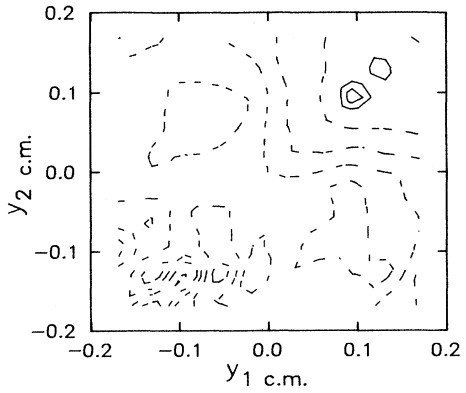

FIG. 1. A contour plot of $\langle \mathbf{p}^{\perp}(y_1) \cdot \mathbf{p}^{\perp}(y_2) \rangle / (\langle p^{\perp}(y_1) \rangle \langle p^{\perp}(y_2) \rangle)$ for midcentral C+C collisions as 50 MeV/nucleon. The dashed lines represent negative contour levels, while the solid lines correspond to positive levels.

$$\langle \mathbf{p}^{\perp}(y_1)/A_1 \cdot \mathbf{p}^{\perp}(y_2)/A_2 \rangle = \langle p^x(y_1)/A_1 \rangle \langle p^x(y_2)/A_2 \rangle - \alpha \langle (p^{\perp}/A)^2 \rangle , \quad (3)$$

where α is of the order $1/(M-2)$, M being the multiplicity of emitted fragments. In the cases where M is small or the dynamic collective effects are weak, then the correlation will be negative throughout most of the (y_1, y_2) plane.

We have evaluated the scalar product on the left-hand side of Eq. (3) for data obtained in the reaction $^{12}C + ^{12}C$ at 50 MeV/nucleon. The effect of detector biases (energy thresholds, angular granularity, etc.) is minimized by dividing Eq. (3) throughout by

$$\langle p^{\perp}(y_1)/A_1 \rangle \langle p^{\perp}(y_2)/A_2 \rangle .$$

In the resulting contour plot of the midcentral data (Fig. 1), the average scalar product is negative throughout most of the rapidity space, with the exception of a positive region when both fragments have rapidity $y \simeq +y_{proj}$. Guided by Eq. (3), this contour map indicates that the correlation of transverse momenta is influenced by momentum conservation. The positive region indicates the presence of some weak collective effects.

Danielewicz *et al.*[6] use Eq. (3) to determine the aver-

TABLE I. The gates on midrapidity charge (Z_{mr}) used to select impact-parameter ranges. The mean impact parameter is given in units of $R_{proj} + R_{targ}$.

Reaction	Gate	Z_{mr}	Mean impact parameter
C+C 50 MeV/nucleon	central	$Z \geq 8$	0.25
C+C 50 MeV/nucleon	midcentral	$5 \leq Z < 8$	0.4
C+C 50 MeV/nucleon	midperipheral	$2 \leq Z < 5$	0.6
Ar+V 35 MeV/nucleon	central	$Z \geq 13$	0.25
Ar+V 35 MeV/nucleon	midcentral	$8 \leq Z < 13$	0.4
Ar+V 35 Mev/nucleon	midperipheral	$3 \leq Z < 8$	0.6

age projected transverse momentum $\langle p^x(y)/A \rangle$ by solving a set of three coupled equations. An alternative method is to modify the standard, event-by-event, transverse momentum analysis by correcting for the effects of momentum conservation. In the standard analysis, the projected transverse momentum for fragment i is given by

$$p_i^x = \frac{\mathbf{p}_i^\perp \cdot \mathbf{Q}'}{|\mathbf{Q}'|} , \tag{4}$$

where

$$\mathbf{Q}' = \sum_{\substack{j=1 \\ j\neq i}}^{M} \omega_j \mathbf{p}_j^\perp . \tag{5}$$

The weights ω_j must have opposite signs for forward and backward going fragments. The system that determines the reaction plane ($\mathbf{Q}'$) is moving in the transverse direction with momentum $\mathbf{p}^\perp = -\mathbf{p}_i^\perp$. Applying a boost ($\mathbf{v}_b$) to each fragment j,

$$\mathbf{v}_b = \frac{\mathbf{p}_i^\perp}{m_{\rm sys} - m_i} , \tag{6}$$

means that the system used to evaluate $\mathbf{Q}'$ has no net transverse momentum. Equation (5) becomes

$$\mathbf{Q}' = \sum_{\substack{j=1 \\ j\neq i}}^{M} \omega_j (\mathbf{p}_j^\perp + m_j \mathbf{v}_b) . \tag{7}$$

In these equations m_j is the mass of the emitted fragment and $m_{\rm sys}$ is the sum of the projectile and target masses.

The calculation of the average transverse momentum with Eq. (4) combined with either Eq. (5) or (7) is studied in the following with the data of deuterons emitted in midperipheral collisions of $^{12}C+^{12}C$ at 50 MeV/nucleon. Figure 2 shows the average transverse momentum per nucleon without the correction for momentum conservation [Eq. (5)]. The shape as a function of rapidity is similar to that observed in higher-energy data,[2] but the data are not symmetric in the forward and backward hemispheres. The correction for momentum conservation event by event produces the transverse momentum distribution in Fig. 3. This plot is similar to that in Fig. 2 but displaced vertically in the forward hemisphere by 3.5 MeV/c, equivalent to a 35% change in the magnitude of the forward hemisphere plateau. The remaining asymmetry is due to the low-energy thresholds of the 4π array. This causes an incomplete coverage of the transverse momentum distribution near and below $y_{\rm c.m.}=0$, which biases the calculation of average quantities. This effect is reduced when calculating the fraction of the fragment's perpendicular momentum that lies in the reaction plane, i.e., $\langle p^x/p^\perp \rangle$.

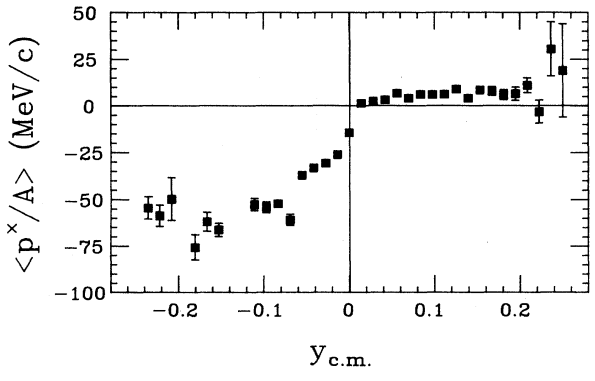

FIG. 2. The average transverse momentum per nucleon as a function of center-of-mass rapidity for deuterons emitted in midperipheral C+C collisions at 50 MeV/nucleon. The transverse momentum has been calculated without the recoil correction.

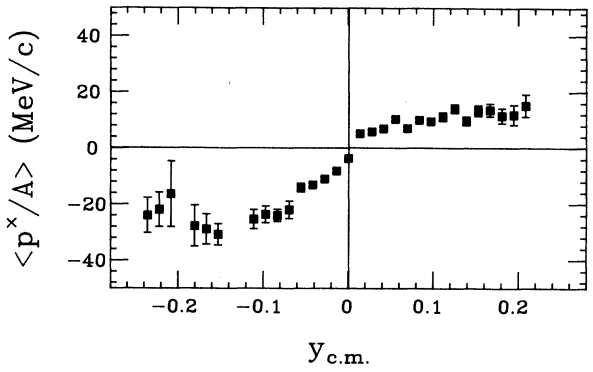

FIG. 3. The same as for Fig. 2 but including the recoil correction.

We have generated Monte Carlo events without any collective effects in the reaction plane, but constrained by momentum conservation. These were filtered through a software replica of the 4π array, and produced a flat, but negative transverse momentum when no corrections were used [Eq. (5)]. Application of the event-by-event momentum correction [Eq. (7)] produced a flat and zero transverse momentum within statistical errors.

To find a optimum weighting factor ω_j, we have randomly divided every event into two halves and calculated the vector $\mathbf{Q}$ for each half,

$$\mathbf{Q} = \sum_{j}^{M/2} \omega_j \mathbf{p}_j^\perp . \tag{8}$$

In Fig. 4 we plot the distribution of azimuthal angle between the two half-event vectors $\mathbf{Q}$ for $^{12}C+^{12}C$ midperipheral events, where at least one fragment from the event is in the backward center-of-mass hemisphere. The distribution has a peak at 0°, which testifies to the presence of some collective motion in the reaction plane. The removal of the requirement that at least one fragment is in the backward hemisphere broadens the distribution; a result consistent with the influence of momentum conservation.

Figure 4 is the optimized distribution of the azimuthal angle with the weights ω_j chosen to be

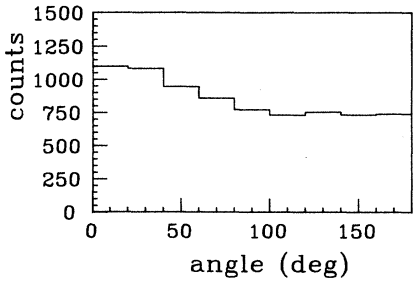

FIG. 4. The distribution of the difference between azimuthal angles for the two half-event Q vectors for C+C midcentral events at 50 MeV/nucleon.

$$\omega_j = m_j \text{ if } y_j > 0$$
$$= -m_j \text{ if } y_j < 0 ,$$

where m_j is the mass of the fragment. It is expected[2] that the dispersion ($\Delta\phi$) of Q with respect to the reaction plane should be half the width of this distribution. Such a dispersion dampens the measured transverse momentum by approximately $\cos(\Delta\phi)$. This factor is often determined from plots such as Fig. 4 and then used to renormalize the measured transverse momentum. However, when the collective effects are weak the method is likely to be inaccurate. A better comparison to theory may be made by insisting that theoretical calculations determine the transverse momentum with the found, instead of known, reaction plane.

In the next section we present only nonrenormalized results. For completeness we calculate an estimated renormalization factor using a method first introduced by Danielewicz and Odyniec and refined by Zhang and Keane.[7] The event-average total transverse momentum per fragment within the found reaction plane is

$$\overline{\omega P^x_{\text{found}}} = \frac{\overline{\sum_{i=1}^{M} \omega_i p_i^x}}{\overline{M}} , \tag{9}$$

where $\overline{M}$ is the average multipliticity of the events. The average size of the vector Q is given by

$$Q^2 = \overline{\sum_{i=1}^{M} \omega_i \mathbf{p}_i^{\perp} \cdot \mathbf{Q}'} , \tag{10}$$

Where Q′ is found using Eq. (7). The event-average total transverse momentum per fragment within the true reaction plane can be estimated from Q^2

$$\overline{\omega P^x_{\text{true}}} = \left[\frac{Q^2}{\overline{M}(\overline{M}-1)} \right]^{1/2} . \tag{11}$$

Taking the ratio of Eqs. (9) and (11) provides an estimate of the renormalization factor.

IV. RESULTS

A. $^{12}C+^{12}C$ at 50 MeV/nucleon

Figure 5 shows the in-plane fraction of transverse momentum as a function of center-of-mass rapidity for protons, deuterons, tritons, He, and Li fragments emitted in central, midcentral, and midperipheral C+C collisions at 50 MeV/nucleon. Transverse collective motion is observed for all fragment types. It is weakest for protons and increases in strength with the mass of the fragment.

TABLE II. The mean of the in-plane fraction of transverse momentum and the projected transverse momentum per nucleon for C+C at 50 MeV/nucleon. The mean is taken over the rapidity intervals indicated in the text. For each quantity the error represents the standard deviation from the mean, while the last column is the systematic uncertainty for that fragment type. The estimated renormalization factor is given for each impact parameter bin.

	Central	Midcentral	Midperipheral	Systematic
		$\overline{\langle p^x/p^{\perp} \rangle}$		
Protons	0.076±0.004	0.078±0.003	0.072±0.002	0.004
Deuterons	0.064±0.010	0.081±0.006	0.087±0.004	0.004
Tritons	0.10±0.04	0.13±0.01	0.126±0.007	0.01
$Z=2$	0.21±0.02	0.199±0.005	0.171±0.003	0.04
$Z=3$	0.25±0.11	0.22±0.02	0.24±0.01	0.05
Renormalization	$1.7\pm^{0.3}_{0.2}$	$2.0\pm^{0.4}_{0.3}$	$2.3\pm^{0.5}_{0.4}$	
		$\overline{\langle p^x/A \rangle}$ (MeV/c)		
Protons	8.5±0.6	8.6±0.4	8.2±0.3	0.4
Deutrons	7.9±1.2	9.4±1.2	10.1±0.7	0.4
Tritons	13.3±4.0	14.2±1.0	13.5±0.6	0.5
$Z=2$	15.6±0.9	14.6±0.3	12.1±0.2	2.5
$Z=3$	20.2±6.0	16.0±2.5	17.2±0.4	3.5
Renormalization	$1.7\pm^{0.3}_{0.2}$	$2.0\pm^{0.4}_{0.3}$	$2.3\pm^{0.5}_{0.4}$	

The collective motion is similar for each of the impact-parameter groups. Due to the low-energy thresholds and the coarse angular acceptance of the detectors, the slope of the distribution at $y_{\text{c.m.}}=0$ is not the most reliable quantity to extract from our data. Instead, we introduce the quantities $\langle p^x/p^\perp \rangle$ and $\langle p^x/A \rangle$ which are the means of the corresponding distributions in the rapidity range $0.3y_{\text{beam}} < y < y_{\text{beam}}$. This region is indicated by arrows in Fig. 5. The results for C+C are listed in Table II. The error in each column is the standard deviation about the mean value, while the error in the final column is the systematic error. The latter have been estimated by using different ranges of rapidities in calculating the averages. An additional error is included for the $Z=2$ and $Z=3$ groups due to the lack of isotopic identification. For completeness, we have included an estimate of the renormalization factor found from the ratios of Eqs. (9) and (11). Qualitatively similar results for the dependence on the emitted fragment were found when the data were analyzed without the correction for momentum conservation.

B. ^{40}Ar+^{51}V at 35 MeV/nucleon

In Fig. 6 we plot the in-plane fraction of transverse momentum for Ar+V collisions at 35 MeV/nucleon. There is no statistically significant collective motion observed for the protons and deuterons. Collective motion is observed for tritons and is present to a greater extent for helium and lithium fragments. There is no significant evidence that the collective motion is different for the three impact-parameter bins. The results for the Ar+V collisions are summarized in Table III. Qualitatively similar results for the dependence on the emitted fragment were found when the data were analyzed without the correction for momentum conservation.

V. COMPARISON TO OTHER WORK

As mentioned in the Introduction, a transition between negative angle scattering and positive angle scattering is expected to take place in heavy-ion collisions at some beam energy below 200 MeV/nucleon. Such a change of

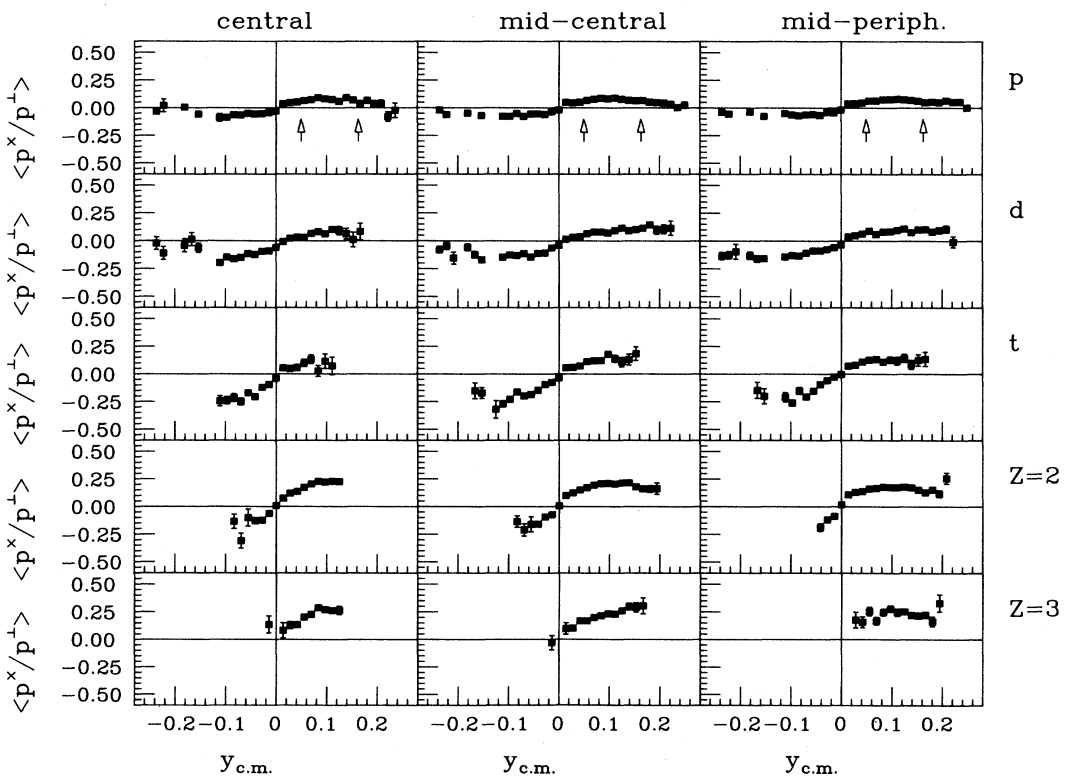

FIG. 5. The in-plane fraction of transverse momentum as a function of center-of-mass rapidity for fragment's emitted in C+C collisions at 50 MeV/nucleon. The columns correspond to central, midcentral and midperipheral collisions, respectively. The rows correspond to protons, deuterons, tritons, $Z=2$ and $Z=3$ fragments, and the arrows correspond to the rapidity ranges used to calculate average quantities.

TABLE III. Same as for Table II but for Ar+V at 35 MeV/nucleon.

	Central	Midcentral	Midperipheral	Systematic
		$\overline{\langle p^x/p^\perp \rangle}$		
Protons	0.004±0.005	−0.001±0.002	−0.006±0.002	0.002
Deuterons	0.006±0.006	0.002±0.004	0.001±0.003	0.004
Tritons	0.03±0.02	0.031±0.006	0.020±0.004	0.005
$Z=2$	0.054±0.010	0.052±0.005	0.046±0.004	0.012
$Z=3$	0.057±0.008	0.069±0.008	0.061±0.006	0.013
Renormalization	$3.4\pm^{1.0}_{0.6}$	$3.3\pm^{0.9}_{0.7}$	$3.6\pm^{0.9}_{0.7}$	
		$\overline{\langle p^x/A \rangle}$ (MeV/c)		
Protons	1.1±0.6	0.4±0.3	−0.3±0.3	0.1
Deuterons	1.6±0.8	0.6±0.5	0.4±0.3	0.4
Tritons	4.1±1.9	3.9±1.0	2.5±0.5	0.6
$Z=2$	4.4±0.9	4.2±0.4	3.9±0.3	0.9
$Z=3$	5.9±0.8	6.7±0.9	6.0±0.5	1.1
Renormalization	$3.4\pm^{1.0}_{0.6}$	$3.3\pm^{0.9}_{0.7}$	$3.6\pm^{0.9}_{0.7}$	

reaction mechanism might be observed if we examined the magnitude of the transverse momentum at different beam energies. In Fig. 7 we plot the reduced quantities

$$\frac{\overline{\langle p^x/A \rangle}}{p_{\text{proj}}/A}$$

for a variety of systems at different beam energies. The scaling factor,[8] p_{proj}/A, is the momentum per nucleon of the projectile in the center-of-mass frame of the nuclei. Our data have been extracted from midcentral collisions, averaged over all fragment types detected, and have been renormalized by the factors in Tables II and III. The other data shown are from experiments performed by the

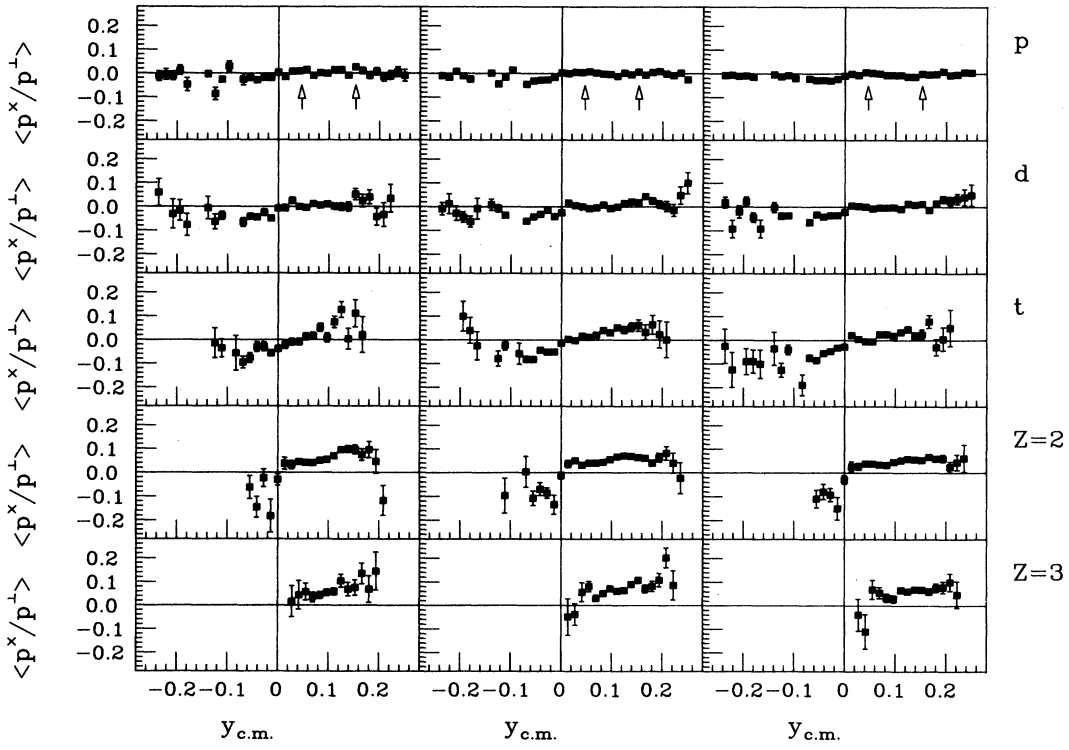

FIG. 6. The same as for Fig. 5 but for Ar+V collisions at 35 MeV/nucleon.

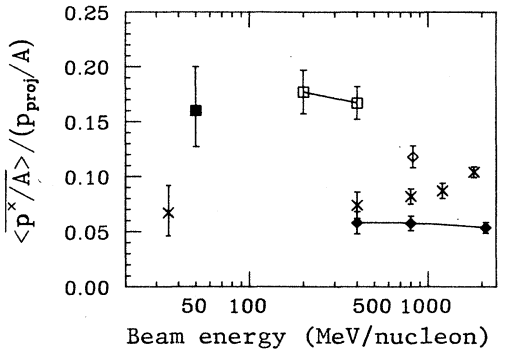

FIG. 7. The reduced transverse momentum per nucleon for a variety of systems over a range of bombarding energies. The two lowest-energy points are our data presented in this paper; the solid square is from C+C and the cross is from the Ar+V data. The error bars include both systematic and statistical errors. The crosses at higher energies are from Ar+KCl, and Ca+Ca reactions performed by two GSI/LBL groups (Refs. 2, 6, and 9). The solid diamonds represent Ne+NaF collisions (Ref. 10), the open squares Au+Au collisions (Ref. 9), and the open diamonds La+La collisions (Ref. 6). The lines join the data for each system and are drawn to guide the eye.

Streamer Chamber and Plastic Ball groups.[2,6,9,10] There exist other data down to 200 MeV/nucleon;[11] however, the published results only provide the slope of the transverse momentum at zero rapidity (the "flow"). From Fig. 7 it is apparent that our Ar+V data are consistent with the transverse motion observed at higher energies. The fact that the C+C data show somewhat stronger collective effects than the Ar+V data possibly indicates that the transverse momentum has a different projectile mass dependence than that observed at higher energies. It is clear that a more systematic study (different systems at several beam energies) is needed before we can ascertain whether a change of mechanism has occurred.

VI. DISCUSSION AND CONCLUSIONS

We have measured the reactions $^{40}Ar+^{51}V$ at 35 MeV/nucleon and $^{12}C+^{12}C$ at 50 MeV/nucleon with the MSU 4π array. The observed correlations between the fragment's transverse momenta are affected by the constraint of momentum conservation with some evidence for weak collective effects. The global transverse momentum analysis was therefore modified to include a recoil correction.

With the event-by-event recoil correction, transverse collective motion has been observed for all fragment types detected. The data have not been renormalized to account for the inaccuracy in determining the reaction plane, because the standard technique for doing this leads to large systematic errors when the collective effects are weak. It is also argued that for our data $\langle p^x/p^\perp \rangle$ is influenced less by the detector thresholds than is $\langle p^x/A \rangle$. Similarly, $\langle p^x/p^\perp \rangle$ is less influenced by the coarse angular acceptance and low-energy thresholds than the "flow" at zero rapidity.

The values of $\langle p^x/p^\perp \rangle$ indicate that the collective effects are stronger for heavier fragments. The transverse momentum is similar for each of the impact-parameter groups. The collective motion in C+C is stronger than in Ar+V.

The nonzero directed transverse momentum implies that the emission of fragments is nonisotropic in the transverse direction. We therefore cannot represent the reaction as producing a single source at equilibrium, since a source with relaxed kinetic degrees of freedom would produce an isotropic distribution of fragments. In many thermodynamic analyses of heavy-ion reactions, the slopes of measured kinetic energy spectra are used to deduce an apparent temperature of the emitting source. These spectra are a complicated superposition of thermal and collective motion in the source. On the basis of our results, a large fraction (up to 25% for heavier fragments) of the fragment's perpendicular momentum appears to be collective in nature. This collective component should be subtracted in some way from the energy spectra before an apparent kinetic temperature can be deduced.

A future comparison of our data with the predictions of microscopic dynamical models (Vlasov-Uhling-Uhlenbeck[12] and quantum molecular dynamics[13]) should provide insight into the reaction mechanism that produces the collective motion. Such a comparison may help determine how accurately these models describe nuclear collisions. In the meantime, a comparison with higher-energy results indicates that the projectile dependence of the transverse momentum may be different at low energies. However, more systematics are needed before we can ascertain whether the collective motion is due to attractive mean-field effects or related to the hydrodynamic phenomena studied at higher beam energies.

ACKNOWLEDGMENTS

The authors thank Professor Wolfgang Bauer and David Krofcheck for stimulating discussions. This work was supported in part by the National Science Foundation under Grant No. PHY-86-11210.

*On leave of absence from the Institute of Theoretical Physics, Warsaw University, Warsaw, Poland.

†Permanent address: University of Michigan, 4901 Evergreen Road, Dearborn, MI 48128.

[1]C. K. Gelbke and D. H. Boal, Prog. Part. Nucl. Phys. **19**, 33 (1987).

[2]P. Danielewicz and G. Odyniec, Phys. Lett. **157B**, 146 (1985).

[3]J. J. Molitoris, D. Hahn, and H. Stocker, Nucl. Phys. **A447**, 13c (1985).

[4]G. D. Westfall, J. E. Yurkon, J. van der Plicht, Z. M. Koenig, B. V. Jacak, R. Fox, G. M. Crawley, M. R. Maier, B. E. Hasselquist, R. S. Tickle, and D. Horn, Nucl. Intrum. Methods **A238**, 347 (1985).

[5]C. A. Ogilvie, D. A. Cebra, S. Howden, J. Karn, A. Vander

Molen, G. D. Westfall, W. K. Wilson, and J. S. Winfield, Phys. Rev. C **40**, 654 (1989).
[6]P. Danielewicz, H. Strobele, G. Odyniec, D. Bangert, R. Bock, R. Brockmann, J. W. Harris, H. C. Pugh, A. Sandoval, L. S. Schroeder, and R. Stock, Phys. Rev. C **38**, 120 (1988).
[7]W. Zhang and D. Keane (private communication).
[8]A. Bonasera, L. P. Csernai, and B. Schurmann, Nucl. Phys. **A476**, 159 (1988).
[9]H. A. Gustafsson, H. H. Gutbrod, J. Harris, B. V. Jacak, K. H. Kampert, B. Kolb, A. M. Poskanzer, H. G. Ritter, and H. R. Schmidt, Mod. Phys. Lett. **A3**, 1323 (1988).
[10]M. Vient, Ph.D. thesis, University of California, Riverside, 1988.
[11]K. G. R. Doss, H. A. Gustafsson, H. H. Gutbrod, K. H. Kampert, B. Kolb, H. Lohner, B. Ludewigt, A. M. Poskanzer, H. G. Ritter, H. R. Schmidt, and H. Weiman, Phys. Rev. Lett. **57**, 302 (1986).
[12]G. F. Bertsch and S. das Gupta, Phys. Rep. **160**, 189 (1988).
[13]G. Peilart, H. Stocker, W. Greiner, A. Rosenhauer, A. Bohnet, and J. Aichelin, Phys. Rev. C **39**, 1402 (1989).